Inorganic Chemistry

Article

pubs.acs.org/IC

A Coordination Complex System for Generic, Ultrafast, and Sensitive Multimode Fluorescent Staining of Biomolecules

Xingqiang Liu, Lingjuan Li, Jingjing Sun, Yishu Yan, Xin Shu, Baoqing Liu, Wei Sha, Hui Feng, Sha Sun, and Jin Zhu*

Department of Polymer Science and Engineering, School of Chemistry and Chemical Engineering, State Key Laboratory of Coordination Chemistry, Nanjing National Laboratory of Microstructures, Nanjing University, Nanjing 210093, China

Supporting Information

ABSTRACT: Gel electrophoresis staining methodologies documented thus far are largely utilized in a biomolecule context-dependent manner. We report herein the development of a generic, ultrafast, and sensitive multimode fluorescent system for the efficient identification of DNA, RNA, and proteins. Interaction between a positively charged, planar ligand-based coordination complex with partner biomolecule leads to aggregation-induced fluorescence quenching and allows for the image contrast generation within one minute. Alternatively, successive reactions of the biomolecule-loaded gel with cation and ligand, in either order of sequence, provide an equally effective staining efficacy. Image contrast reversal is accomplished through a facile washing or photobleaching procedure. The versatility in the applicable target species and signal generation modes provides a hint at the design of novel staining structures and potentially enables the high-throughput readout of biomolecules.

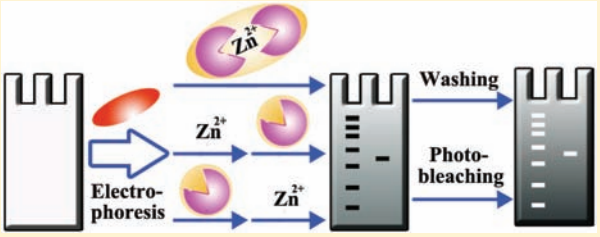

INTRODUCTION

The complex and dynamic nature of the biological entities inside cells commands a system-wide genomics and proteomics approach to the analysis of networked architectures.[1] The formidable undertaking has prompted the establishment of new arsenal of experimental techniques for the efficient characterization of molecular structures. Indeed, expeditious detection is prerequisite to the effective coverage of a sufficient number of biologically relevant species in a comprehensive study that is urgently required for a more complete understanding of sophisticated cellular and physiological processes. With these challenges in mind and building upon our expertise in biodiagnostics,[2] herein, we wish to report on the development of an ultrafast fluorescent staining system for the identification of biomolecules in gel electrophoresis. Gel electrophoresis,[3] a technique for the separation of biological species based on the electric field-driven migration of charged objects, is arguably one of the most valuable tools in life sciences. The visualization of biomolecule bands in the gel matrix relies on the generation of a contrast image through the nonuniform distribution of a readout species.[4] The signal registered from such a spatially selective deposition of the contrast reagent could derive from organic dyes, fluorescent molecules, silver stain, radioactive labels, and inorganic salts. In spite of tremendous success, the staining methodologies reported thus far remain largely utilized in a biomolecule context-dependent manner. For example, traditionally, the detection of nucleic acids and proteins is generally considered distinctly different and therefore typically achieved with structurally disparate reagents. Nucleic acids are generally visualized through the intercalation-driven fluorescence enhancement[5] whereas proteins are imaged usually through electrostatic interaction-based binding of organic dyes.[6] The merger of the detection methods for these two classes of molecules[4a,b] could potentially allow for the integration of an information acquisition platform for genomics and proteomics research under certain circumstances. Our approach to the achievement of an unbiased signal readout is the establishment of a generic, speedy, and sensitive multimode fluorescent staining system for the identification of DNA (both single-stranded and double-stranded), RNA, and proteins.

RESULTS AND DISCUSSION

The design of our coordination complex-based staining scheme takes into account several key considerations: (1) The molecular coordination site should be devoid of negatively charged functional groups (e.g., carboxylic group) so that the positive charge on the cation is not neutralized upon the complex formation and electrostatic interaction can contribute to the binding with target biomolecule. (2) The immediate molecular surroundings of the coordination site should not be too bulky, otherwise electrostatic interaction could be blocked. (3) The molecule should possess an extended structure so that extensive contact with target biomolecule can confer effective interaction force. (4) The molecular framework should not contain excessively strong basic groups (e.g., primary amino group) so that the photophysical properties are not substantially affected by the variation of pH and the probe is

Received: July 5, 2011
Published: December 6, 2011

   dx.doi.org/10.1021/ic201406b | Inorg. Chem. 2012, 51, 188–192

robust toward the uncertainty in the pH settings. (5) The cation-binding behavior of the molecule should be highly selective so that interference from other cations is minimized and the broad applicability of the probe is guaranteed. (6) The molecule should possess a low aqueous solubility and therefore a low dose of potential hazard, if any, would be exposed to living cells/organisms, but the staining process should still be allowed to proceed in a highly efficient manner in the complex format. The fluorescent system selected herein that fulfills the above requirements features a planar heterocyclic conjugate structure, dipyrido[3,2-*a*:2′,3′-*c*]thien[3,4-*c*]azine (**Z1**),[7,8] which, when in association with Zn^{2+}, forms a desired complex in the 2:1 ratio ($[Zn{\cdot}\mathbf{Z1}_2]^{2+}$) (Figure 1). Significantly, the

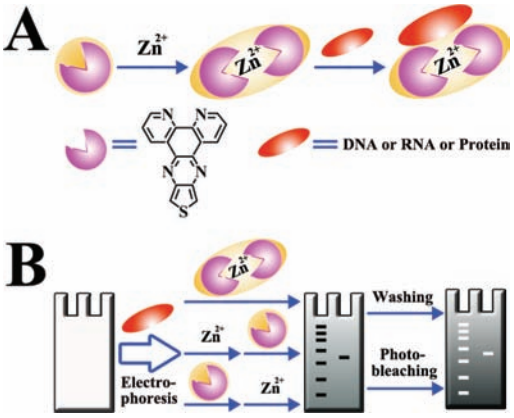

Figure 1. Schematic representation of the generic, ultrafast, and sensitive multimode fluorescent staining of biomolecules in gel electrophoresis. (A) Coordination complex formation between the fluorescent molecule **Z1** and Zn^{2+} ($[Zn{\cdot}\mathbf{Z1}_2]^{2+}$), and binding with biomolecules (DNA, RNA, or protein). Molecule **Z1** possesses a planar heterocyclic conjugate structure and could interact with Zn^{2+} through the dipyrido chelation site. Both Zn^{2+} and **Z1** contribute to the binding with biomolecules. (B) Image contrast generation in gel electrophoresis through the fluorescent staining of biomolecule bands with the $[Zn{\cdot}\mathbf{Z1}_2]^{2+}$ complex. The dark biomolecule bands (with lower fluorescence relative to the gel matrix), derived from aggregation-induced fluorescence quenching, could be observed upon incubation of the gel matrix in the $[Zn{\cdot}\mathbf{Z1}_2]^{2+}$ staining solution for merely one minute, or through successive reactions with Zn^{2+} and **Z1** in either order of sequence. The image contrast reversal and observation of bright bands could be achieved through either a simple washing procedure, enabled by the tightly bound residual fluorescent $[Zn{\cdot}\mathbf{Z1}_2]^{2+}$ complex, or a facile photobleaching process, effected by selectively more severe reduction of the fluorescence intensity in the biomolecule-free background area under extended UV light irradiation.

ultrafast staining can be accomplished within one minute through the generation of image contrast (dark band, negative staining) by the selective deposition of $[Zn{\cdot}\mathbf{Z1}_2]^{2+}$ and aggregation-induced fluorescence quenching in the biomolecule-loaded zone. Alternatively, successive incubation of the electrophoresed gel in Zn^{2+} and **Z1** solutions, in either order of reaction sequence, provides an equally effective staining efficacy. The dark band produced therein could be reversed to a bright reporter signature (positive staining) through either washing-based removal of the majority of $[Zn{\cdot}\mathbf{Z1}_2]^{2+}$ aggregate in the biomolecule-loaded area and concomitant lighting up by the remaining tightly bound fluorescent species, or the selective more severe photobleaching (destruction of fluorescence) of $[Zn{\cdot}\mathbf{Z1}_2]^{2+}$ complex in the biomolecule-free background area with extended UV light irradiation. The multifaceted staining capability provides evidence that both Zn^{2+} (through electrostatic interaction) and **Z1** (likely through van der Waals interaction) play a role in the association between the coordination complex and analyte structure. The versatility in the applicable target species and signal generation modes could provide a hint at the design of novel staining structures and potentially enable the high-throughput readout of biomolecules. Although an imidazole–Zn^{2+} complex has been previously used for the staining of biomolecules in both the negative and positive modes,[4b,c] the system is based on the contrast generation from optical absorption signature.

Z1 was synthesized in five steps starting from thiophene and phenanthroline, and fully characterized with ^1H and ^{13}C nuclear magnetic resonance (NMR) spectroscopy, matrix-assisted laser desorption/ionization time-of-flight mass spectrometry (MALDI-TOF MS), high-resolution MS (HRMS), and elemental analysis (Figures S1–S8 and Table S1 in the Supporting Information (SI)).[7] As expected, due to the extended conjugation structure, **Z1** is only barely soluble in a variety of solvents. However, one prominent feature of the molecule is the existence of a nitrogen-based chelation site on the dipyrido moiety, the cation coordination of which would render it positively charged and substantially improve the solubility, in polar solvents in particular. Guided by the consideration that the preparation procedure for the **Z1** complex should be straightforward and inexpensive, we have set out to evaluate the binding capacity of **Z1** toward a variety of cations at ambient conditions. The challenge of an aqueous suspension of **Z1** with 17 types of cations allows the identification of Zn^{2+} as the sole binding-capable species (Figures S9–S11 in the SI). Indeed, the continued addition of Zn^{2+} to the precipitate-loaded **Z1** suspension leads to the appearance of a greenish yellow solution with the concomitant increase of absorbance and fluorescence intensity. The increase in the solubility of **Z1** upon the Zn^{2+} binding is primarily responsible for the change in both the visual outlook and photophysical properties. The broad and unstructured emission band is reminiscent of the intramolecular charge transfer (ICT) character of the excited singlet state.[9] In support of this, a red shift of the emission maximum has been observed upon the increase of the solvent polarity (Figure S12 in the SI).[9] In addition, the existence of an ICT state for both **Z1** and **Z1** complex (for optimized geometries, see Figures S13 and S14 in the SI) has also been verified by time-dependent density functional theory (TDDFT) calculations (Figures S15 and S16 in the SI). The peak positions of both absorption and emission spectra are determined by the energies of relevant ground and excited electronic states of **Z1** and Zn^{2+}-bound **Z1**. This is in turn dictated by the competing stabilization force of hydrogen bonding (from protic polar solvent) and coordination interaction (from complexed Zn^{2+}) for the respective ICT state. Due to the lack of strong basic sites in the rigid planar structure, the fluorescence of **Z1** remains largely unaffected over a wide pH window (Figure S17 in the SI). Besides the solubility and spectroscopic evidence, the ability of **Z1** to interact with Zn^{2+} was further supported by the NMR titration (Figure S18 in the SI) and electrospray ionization MS (ESI-MS) experiments (Figure S19 in the SI). All the aromatic and thiophene proton peaks of **Z1** were broadened and showed evident downfield shift changes upon the addition of Zn^{2+}, attributable to the deshielding effect arising from the decrease of electron density caused by Zn^{2+} binding of the conjugate structure. Importantly, the ESI-MS experiment allowed the

dx.doi.org/10.1021/ic201406b | *Inorg. Chem.* 2012, 51, 188–192

observation of two charged species, [**Z1** + Zn^{2+} + CH_3COO^-] and [2**Z1** + Zn^{2+} + CH_3COO^-], with the expected isotopic peaks derived from the Zn element. No $[Zn{\cdot}\mathbf{Z1}_3]^{2+}$-related species could be identified by MS in a mixture of **Z1** and Zn^{2+} containing an excessive amount of **Z1** (10:1 **Z1**/Zn^{2+} in molar ratio), suggesting the likely absence of higher-numbered ligand configuration. Titration of Zn^{2+} into a completely soluble **Z1** in a 3:1 H_2O/EtOH solvent mixture was examined (Figure S20 in the SI). The clear isosbestic point identified in the titration experiment implies the conversion of free **Z1** to a Zn^{2+}-containing structure. Binding analysis with the continuous variation method (Job's plot) (Figure S21 in the SI) indicates the formation of a 2:1 **Z1**/Zn^{2+}complex.[10] The binding constant as calculated from the UV–vis absorption titration experiment equals 4.3×10^9 M^{-2} in this solvent mixture medium, suggesting the strong binding between the two types of chemical species. The extinction coefficients and quantum yields of **Z1** and $[Zn{\cdot}\mathbf{Z1}_2]^{2+}$ have been quantitatively measured (Tables S2 and S3 in the SI) and provide evidence for their high probe efficacy. The bulky size and unique electronic property of the ligand **Z1** are believed to contribute to the formation of a distinct bis-coordination structure as compared to previously reported cases (e.g., tris(phenanthroline)–Zn^{2+} complex[11a] or dynamic, thermodynamic mixture[11b]).

The staining of biomolecules in gel electrophoresis requires the exquisite interplay of various components to maximize the imaging efficiency. The primary factor controlling the image contrast generation is the differentiated deposition of $[Zn{\cdot}\mathbf{Z1}_2]^{2+}$ complex in the biomolecule zone as compared with the background gel matrix. Key requirements for the high staining efficacy are as follows: fast diffusion of Zn^{2+}/**Z1** into the gel matrix, tight binding between the staining component and target analyte, maintenance of the gel quality, and preservation of the sharp biomolecule band. The achievement of the above requirements relies on, first and foremost, the proper choice of a solvent medium. A pure aqueous solution is not ideal for the robust entrapment of the biomolecule (e.g., diffusion away of DNA from the original band region upon extended incubation). Soaking in a pure alcohol solution would make the gel matrix hardened and brittle. We envisioned that merger of the desired properties of the two solvents is necessary to provide a compelling staining outcome. A careful evaluation of the staining efficacy indicates that the performance of a 2:1 binding complex of **Z1** and Zn^{2+} in 3:1 H_2O/EtOH is satisfactory. The utility of Zn^{2+}/**Z1** in the gel staining process can be better achieved with a higher concentration of the complex. To this end, an initial insoluble **Z1** suspension can be converted to a completely soluble fluorescent species upon the addition of Zn^{2+} (Figure S22 in the SI). With the staining system in hand, we next examined the feasibility of biomolecule detection in the gel electrophoresis experiment. Remarkably, incubation of the gel matrix after the DNA electrophoresis for only one minute results in the appearance of dark bands (in the grayscale fluorescent imaging mode) under the illumination of 312 nm UV light (Figure S23A in the SI). The ability to accomplish the identification of DNA within one minute was confirmed by a time course study of the signal generation process (Figures S24 and S25A–I in the SI). The intensity of the dark bands stays essentially constant after an extremely short period of incubation. The mechanism behind the creation of such an image contrast was rationalized by the simultaneous observation of greenish yellow bands by the naked eye (Figure 2A). Apparently, the preferred deposition of $[Zn{\cdot}\mathbf{Z1}_2]^{2+}$

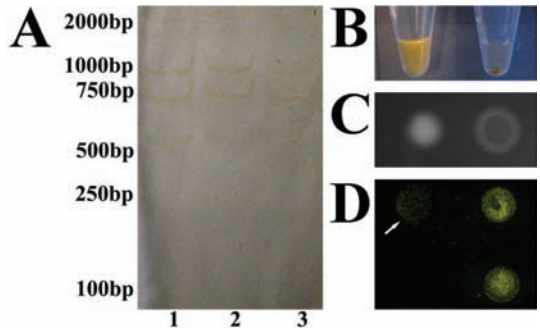

Figure 2. Evidence for the complex aggregation-based, fluorescence quenching-derived ultrafast staining mechanism. (A) Direct visualization of the greenish yellow DNA marker bands. Following the polyacrylamide gel electrophoresis (PAGE), the bands became visible to the naked eye after 1 min incubation of the gel matrix in **Z1** and Zn^{2+}, which was accompanied by the simultaneous appearance of fluorescent dark bands under 312 nm light excitation. Lane 1: 250 ng. Lane 2: 50 ng. Lane 3: 10 ng. (B) Visual outlook of a solution containing either Zn^{2+}/**Z1** (left) or with additional single-stranded **DNA1** (right) under 365 nm light excitation (the image was taken with a colored camera). Precipitate could be clearly identified resulting from the interaction of $[Zn{\cdot}\mathbf{Z1}_2]^{2+}$ with DNA. (C) Fluorescence images of a solution containing **Z1**, Zn^{2+}, and single-stranded **DNA1** in the solution (left) and dried (right) state (the image was taken with an image analysis system). (D) Fluorescence images of a glass slide after first modification with single-stranded **DNA2** (top right), subsequent hybridization with a complementary **DNA1** (bottom right), and eventual incubation in **Z1** and Zn^{2+}. The color on the fluorescence image was arbitrarily selected. The white arrow-designated area was used as a control with no DNA derivatized.

complex in the biomolecule-loaded zone leads to the aggregation-induced fluorescence quenching (Figure 2B,C). Presumably, fast diffusion of EtOH into the gel matrix and its entrapment/immobilization of the biomolecule, coupled with subsequent speedy, selective accumulation of $[Zn{\cdot}\mathbf{Z1}_2]^{2+}$ complex, lead to the achievement of ultrafast imaging. The reversal of the image contrast could be accomplished through a simple washing procedure (Figure S23B in the SI), enabling the appearance of bright bands for the target identification. The emergence of the bright bands under these conditions is derived from the residual $[Zn{\cdot}\mathbf{Z1}_2]^{2+}$ bound to the biomolecule, as evidenced by the observation of extremely faint bands by the naked eye. Alternatively, the bright bands could be generated by a photobleaching process (Figure S25J–L in the SI), where continued UV light irradiation causes selectively more severe reduction of the fluorescence intensity of $[Zn{\cdot}\mathbf{Z1}_2]^{2+}$ complex in the biomolecule-free gel matrix area. Apparently, the different photobleaching propensity of $[Zn{\cdot}\mathbf{Z1}_2]^{2+}$ is imparted by the distinct dispersed state of the complex in the biomolecule-loaded zone as compared with the background region. The staining process is not significantly influenced by the prior incubation of gel in buffer and salt solutions (Figure S26 in the SI). The nature of the binding mode between $[Zn{\cdot}\mathbf{Z1}_2]^{2+}$ and DNA was preliminarily investigated by the fluorescence microscopy examination of $[Zn{\cdot}\mathbf{Z1}_2]^{2+}$ adsorption behavior toward the covalently derivatized single- and double-stranded DNA on a glass slide (Figure 2D). The surface-bound DNA monolayer structure provides a relatively well-defined, clean molecular environment for the elucidation of interaction patterns without the interference from the complex gel matrix. The absence of apparent difference in the fluorescence intensity on the two types of DNA spots, as well as the ability of

dx.doi.org/10.1021/ic201406b | *Inorg. Chem.* 2012, 51, 188–192

$[Zn{\cdot}\mathbf{Z1}_2]^{2+}$ system to image proteins (vide infra), provides evidence for the non-intercalation-based binding mechanism. Indeed, fluorescent staining of single- and double-stranded DNA is equally effective under the experimental conditions employed herein (Figure S27 in the SI).

Besides the staining mode through simultaneous incubation in the solution of Zn^{2+} and **Z1** (Figure 3A), the identification of

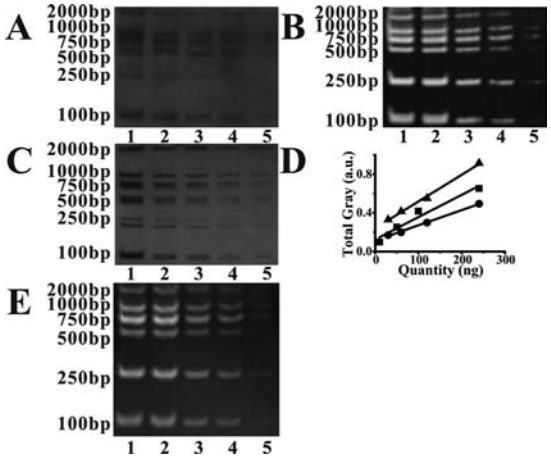

Figure 3. Multimode staining of the Zn^{2+}/**Z1** system for the identification of DNA. (A) Gel electrophoresis diagram of DNA marker in the simultaneous presence of both **Z1** and Zn^{2+}. Lane 1: 240 ng. Lane 2: 120 ng. Lane 3: 60 ng. Lane 4: 30 ng. Lane 5: 15 ng. (B) Gel electrophoresis diagram of DNA marker through a Zn^{2+}-first, **Z1**-second sequential incubation procedure. Lane 1: 240 ng. Lane 2: 100 ng. Lane 3: 50 ng. Lane 4: 10 ng. Lane 5: 2.4 ng. The bright bands are generated through the UV photobleaching process. (C) Gel electrophoresis diagram of DNA marker through a **Z1**-first, Zn^{2+}-second sequential incubation procedure. The quantity of the marker in each lane is the same as that in panel A. (D) Linear relationship between the total gray values (circle, from 2000 bp DNA of image A; square, from 250 bp DNA of image B; triangle, from 2000 bp DNA of image C) and DNA quantities by the three staining protocols. (E) Gel electrophoresis diagram of DNA marker with the ethidium bromide protocol. The quantity of the marker in each lane is the same as that in panel B.

DNA could be accomplished by successive reaction of the biomolecule-loaded gel with Zn^{2+} and **Z1**, in either order of loading sequence (Figure 3B,C). Significantly, even with unoptimized settings, DNA can be detected at a quantity as low as 2.4 ng with our protocol (Figure 3B). Equally important is the quantitative characterization capability of the Zn^{2+}/**Z1** system, as demonstrated by a linear relationship between the total gray values of the DNA bands and DNA quantities (Figure 3D). These attributes are comparable to those achieved by the ethidium bromide method under our experimental conditions (Figure 3E). Control experiments indicate that both **Z1** and Zn^{2+} are required for the creation of an effective staining system for DNA. It is our belief that both the electrostatic interaction (Zn^{2+} with negative backbone of DNA) and $\pi-\pi$ stacking/hydrophobic interaction (**Z1** with nucleotide bases) are responsible for the staining of DNA. Although silver staining might prove useful in certain aspect (e.g., sensitivity) of the gel staining process,[4a] it has its own limitations (such as labor-intensive and time-consuming procedure).

RNA is another important class of biomolecules with fundamentally distinct properties, the study of which could apparently benefit from the imaging capability of our system. The competence of $[Zn{\cdot}\mathbf{Z1}_2]^{2+}$ to generate image contrast for RNA (detection limit under unoptimized conditions: 175 ng) is validated by the equally prompt appearance of dark bands (Figure 4) with image quality comparable to the ethidium

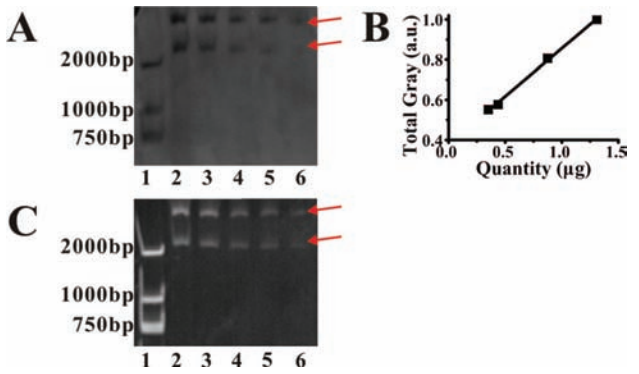

Figure 4. Ultrafast staining of the Zn^{2+}/**Z1** system for the identification of RNA. (A) Gel electrophoresis diagram of extracted RNA products in the simultaneous presence of both **Z1** and Zn^{2+}. Lane 1: DNA marker (240 ng). Lanes 2–6: Extracted RNA products (23S and 16S rRNA) from *Escherichia coli* (BL-21) (red arrows). Lane 2: 1.31 μg. Lane 3: 0.875 μg. Lane 4: 0.438 μg. Lane 5: 0.35 μg. Lane 6: 0.175 μg. (B) Linear relationship between the total gray values (square, from 23S RNA of image A) and RNA quantities. (C) Gel electrophoresis diagram of extracted RNA products with the ethidium bromide protocol. The quantity of RNA in each lane is the same as that in panel A.

bromide method (Figure 4C), and subsequent contrast reversal after the destaining washing step (Figure S23C,D in the SI).

By virtue of the presence of interaction-capable, charged Zn^{2+} and large-sized **Z1**, the present system is envisaged to be applicable to the imaging of proteins. Indeed as expected, the dark and bright bands could be generated through the conceptual framework proposed herein (Figures 5 and S23E,F in the SI), with detection sensitivity (0.05 μg, Figure 5B) and linear quantification capability (Figure 5D) similar to the Coomassie blue protocol (Figure 5E). Both the hydrophobic interaction (**Z1** with hydrophobic amino acids) and electrostatic/coordination interaction (Zn^{2+} with acidic and coordination-capable amino acids) are likely contributing to the staining of proteins. Taken together, compared with the Coomassie blue method, our protocol provides similar staining quality (e.g., signal-to-noise ratio) with a shorter staining time and a multitude of staining modes. In addition, Coomassie blue is not a reagent applicable to the staining of other biomolecules whereas our coordination complex system provides a one-platform staining solution for a diversity of structures. Biomolecular interactions dictate the signal transduction pathways, the analysis of which could benefit from simultaneous visualization of all the interacting partners on one gel. Indeed, our generic staining system allows the identification of DNA and protein concurrently (Figure S28 in the SI) and is therefore anticipated to potentially enable a more in-depth understanding of cellular signaling events.

Mutagenicity is a primary concern for the application of a staining reagent.[12] To exclude such a possibility, the cell permeation capability of $[Zn{\cdot}\mathbf{Z1}_2]^{2+}$ was investigated. Gratifyingly, no apparent penetration of $[Zn{\cdot}\mathbf{Z1}_2]^{2+}$ into the cells could be observed even after prolonged incubation (Figures S29 and S30 in the SI). The lack of cell permeability precludes

dx.doi.org/10.1021/ic201406b | *Inorg. Chem.* 2012, 51, 188–192

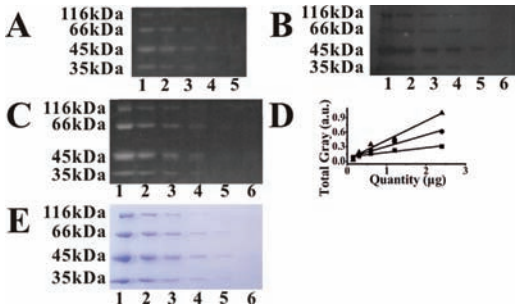

Figure 5. Multimode staining of the Zn^{2+}/**Z1** system for the identification of proteins. (A) Gel electrophoresis diagram of protein marker in the simultaneous presence of both **Z1** and Zn^{2+}. Lane 1: 2.4 μg. Lane 2: 1.2 μg. Lane 3: 0.6 μg. Lane 4: 0.3 μg. Lane 5: 0.15 μg. The bright bands are generated through the UV photobleaching process. (B) Gel electrophoresis diagram of protein marker through a Zn^{2+}-first, **Z1**-second sequential incubation procedure. Lane 1: 2.4 μg. Lane 2: 1.2 μg. Lane 3: 0.6 μg. Lane 4: 0.3 μg. Lane 5: 0.15 μg. Lane 6: 0.05 μg. (C) Gel electrophoresis diagram of protein marker through a **Z1**-first, Zn^{2+}-second sequential incubation procedure. The quantity of the marker in each lane is the same as that in panel B. The bright bands are generated through the UV photobleaching process. (D) Linear relationship between the total gray values (circle, from 45 kDa protein of image A; square, from 116 kDa protein of image B; triangle, from 116 kDa protein of image C) and protein quantities by the three staining protocols. (E) Gel electrophoresis diagram of protein marker with the Coomassie blue protocol. The quantity of the marker in each lane is the same as that in panel B.

the complex from interacting with genomic DNA and therefore renders it nonmutagenic. Further, Ames test has been a widely adopted standard biological assay method for the assessment of mutagenic potential of chemical compounds.[13] One important feature identified through this test is a significantly lower +1 frameshift mutagenic potential (tester strain: *Salmonella typhimurium* TA98; + S9) of the $[Zn{\cdot}\mathbf{Z1}_2]^{2+}$ system as compared with ethidium bromide (2.89 for **Z1**, 1.60 for $[Zn{\cdot}\mathbf{Z1}_2]^{2+}$, 68 for ethidium bromide), with other mutagenic indicators approaching background values.

CONCLUSIONS

In summary, an ultrafast, sensitive multimode fluorescent staining scheme has been developed for the efficient identification of DNA, RNA, and proteins in gel electrophoresis, circumventing the largely biomolecule context-dependent imaging issues for systems documented thus far. Interaction between a positively charged coordination complex and partner target leads to aggregation-induced fluorescence quenching and allows for the signal contrast generation within one minute. The generic gel electrophoresis applicability and versatile signal generation modes of the complex could potentially enable the establishment of novel design principles for biological imaging probes.

ASSOCIATED CONTENT

Supporting Information

Materials and methods, synthetic details, characterization data for all compounds, mechanistic data concerning the complex formation and staining process, and cell permeation properties of the complex. This material is available free of charge via the Internet at http://pubs.acs.org.

AUTHOR INFORMATION

Corresponding Author

*E-mail: jinz@nju.edu.cn.

ACKNOWLEDGMENTS

J.Z. acknowledges support from the National Natural Science Foundation of China (20974044, 90923006) and National Basic Research Program of China (2011CB935801).

REFERENCES

(1) (a) Heard, E.; Tishkoff, S.; Todd, J. A.; Vidal, M.; Wagner, G. P.; Wang, J.; Weigel, D.; Young, R. *Nat. Rev. Genet.* **2010**, *11*, 617−627. (b) Gstaiger, M.; Aebersold, R. *Nat. Rev. Genet.* **2009**, *10*, 723−733. (c) Nilsson, T.; Mann, M.; Aebersold, R.; Yates, J. R. III; Bairoch, A.; Bergeron, J. J. M. *Nat. Methods* **2010**, *7*, 681−685. (d) Mallick, P.; Kuster, B. *Nat. Biotechnol.* **2010**, *28*, 695−709.

(2) (a) Zhou, X.; Xia, S.; Lu, Z.; Tian, Y.; Yan, Y.; Zhu, J. *J. Am. Chem. Soc.* **2010**, *132*, 6932−6934. (b) Zhou, X.; Cao, P.; Tian, Y.; Zhu, J. *J. Am. Chem. Soc.* **2010**, *132*, 4161−4168. (c) Hong, M.; Zhou, X.; Lu, Z.; Zhu, J. *Angew. Chem., Int. Ed.* **2009**, *48*, 9503−9506. (d) Qiu, F.; Jiang, D.; Ding, Y.; Zhu, J.; Huang, L. L. *Angew. Chem., Int. Ed.* **2008**, *47*, 5009−5012.

(3) Westermeier, R. *Electrophoresis in Practice*; Wiley-VCH: Weinheim, 2005.

(4) (a) Bassam, B. J.; Gresshoff, P. M. *Nat. Protoc.* **2007**, *2*, 2649−2654. (b) Castellanos-Serra, L.; Hardy, E. *Nat. Protoc.* **2006**, *1*, 1544−1551. (c) Hardy, E.; Pupo, E.; Casalvilla, R.; Sosa, A. E.; Trujillo, L. E.; López, E.; Castellanos-Serra, L. *Electrophoresis* **1996**, *17*, 1537−1541. and references therein. (d) Miller, I.; Crawford, J.; Gianazza, E. *Proteomics* **2006**, *6*, 5385−5408. (e) Na, N.; Liu, L.; Taes, Y. E. C.; Zhang, C.; Huang, B.; Liu, Y.; Ma, L.; Ouyang, J. *Small* **2010**, *6*, 1589−1592. (f) Wetzl, B. K.; Yarmoluk, S. M.; Craig, D. B.; Wolfbeis, O. S. *Angew. Chem., Int. Ed.* **2004**, *43*, 5400−5402. (g) Meier, R. J.; Steiner, M.-S.; Duerkop, A.; Wolfbeis, O. S. *Anal. Chem.* **2008**, *80*, 6274−6279. (h) Zuchner, T.; Schumer, F.; Berger-Hoffmann, R.; Müller, K.; Lukas, M.; Zeckert, K.; Marx, J.; Hennig, H.; Hoffman, R. *Anal. Chem.* **2009**, *81*, 9449−9453. (i) Suzuki, Y.; Yokoyama, K. *J. Am. Chem. Soc.* **2005**, *127*, 17799−17802. (j) Bell, P. J. L.; Karuso, P. *J. Am. Chem. Soc.* **2003**, *125*, 9304−9305. (k) Smejkal, G. B. *Expert Rev. Proteomics* **2004**, *1*, 381−387. (l) Wallace, A.; Saluz, H. *Nature* **1992**, *357*, 608−609.

(5) (a) Sassolas, A.; Leca-Bouvier, B. D.; Blum, L. J. *Chem. Rev.* **2008**, *108*, 109−139. (b) Klepárník, K.; Boček, P. *Chem. Rev.* **2007**, *107*, 5279−5317.

(6) (a) Wittig, I.; Braun, H.-P.; Schägger, H. *Nat. Protoc.* **2006**, *1*, 418−428. (b) Heinemeyer, J.; Scheibe, B.; Schmitz, U. K.; Braun, H.-P. *J. Proteomics* **2009**, *72*, 539−544. (c) Wittig, I.; Schägger, H. *Proteomics* **2009**, *9*, 5214−5223.

(7) (a) Peng, B.; Chao, H.; Sun, B.; Li, H.; Gao, F.; Ji, L.-N. *J. Inorg. Biochem.* **2007**, *101*, 404−411. (b) Čík, G.; Krajčovič, J.; Veis, P.; Végh, D.; Šeršeň, F. *Synth. Met.* **2001**, *118*, 111−119.

(8) Sammes, P. G.; Yahioglu, G. *Chem. Soc. Rev.* **1994**, *23*, 327−334.

(9) Valeur, B. *Molecular Fluorescence: Principles and Applications*; Wiley-VCH: Weinheim, 2002.

(10) Connors, K. A. *Binding Constants: The Measurement of Molecular Complex Stability*; Wiley-Interscience: New York, 1987.

(11) (a) Barton, J. K.; Dannenberg, J. J.; Raphael, A. L. *J. Am. Chem. Soc.* **1982**, *104*, 4967−4969. (b) Kolthoff, I. M.; Leussing, D. L.; Lee, T. S. *J. Am. Chem. Soc.* **1951**, *73*, 390−394.

(12) Armour, M. A. *Hazardous Laboratory Chemicals Disposal Guide*; CRC Press: Boca Raton, 2003.

(13) Singer, V. L.; Lawlor, T. E.; Yue, S. *Mutat. Res.* **1999**, *439*, 37−47.